JOURNAL OF APPLIED ELECTROCHEMISTRY 9 (1979) 81–87

Electrochemical behaviour and solubility study of hydrogen and acetic acid in molten alkali acetates

R. MARASSI, V. BARTOCCI, M. GUSTERI

Istituto Chimico, Università di Camerino, 62032 Camerino, Italy

P. CESCON

Istituto Chimica Generale, Università di Venezia, Venice, Italy

Received 6 March 1978

The solubility of hydrogen in molten sodium/potassium acetates has been determined in the temperature range 250–300° C. The electrochemical behaviour of hydrogen and acetic acid in the same melt has also been studied at bright platinum electrodes at 250° C.

1. Introduction

Investigations on the electrochemistry of the H^+/H_2 couple in molten salts are relatively few in spite of the possible interest of this couple in connection with fuel cell technology. The hydrogen electrode has been studied in molten carbonates [1–3], fluorides [4], hydroxides [5], chlorides [6–8] and chloroaluminates [9, 10]. Quite recently a potentiometric and voltammetric study of the H_2, OH^-/H_2O half cell in molten nitrates has also been reported [11, 12].

This study, following previous communications [13, 14], deals with the determination of the solubility of molecular hydrogen in the eutectic mixture sodium/potassium acetate (46·3 mol% CH_3COONa) in the temperature range 250–300° C. The electro-oxidation of hydrogen and the reduction of acetic acid have also been studied at 250° C at bright platinum electrodes using different electrochemical techniques.

2. Experimental

The chemicals (CH_3COONa, CH_3COOK and CH_3COOH) were Carlo Erba (Milan) reagent grade and were used without further purification. High purity hydrogen and nitrogen were dried with molecular sieves type 5A before use. The solvent was prepared and handled as described in [14]. The cell used for the voltammetric measurements was a Pyrex vessel connected with the vacuum line by means of an O-ring glass joint. All the electrodes, but the working one, were sealed to the cell body to minimize possible leaks when operating at reduced pressure. Two platinum flags were used as quasi-reference and counter-electrode respectively. The potential of the quasi-reference was measured, when required, versus an Ag^+/Ag (0·07 molal in (Na, K)NO_3 46·3 mol% $NaNO_3$) reference electrode enclosed in a thin glass bulb sealed to the cell body. No attempt was made to measure the junction potential which may be relatively high and change with the type and concentration of solute in the main compartment.

The working electrode was a platinum wire (area about 0·07 cm^2) sealed at the end of a soft glass tube. The electrode was introduced into the cell through an O-ring glass joint and frequently removed for cleaning.

The experimental apparatus for solubility experiments was a modified version of the one described in [14] in which the mercury manometer was adapted for pressure measurements up to 10^2 kPa. The procedure for calibration of the apparatus and for computing the solubility from pressure readings was the same as described in [15].

An AMEL mod 463 multipurpose unit coupled with an *X–Y* (HP 7001 AM) or a HI-TEK AA1 signal averager was used for the electrochemical measurements.

3. Results and discussion

3.1. *Solubility measurements*

The working pressure during the solubility experiments was close to 10^2 kPa. The depression caused by the dissolution process was followed as a function of time by means of the micrometric manometer [14]. A typical example of pressure decay versus time is shown in Fig. 1. The pressure drops relatively fast as soon as the stirring is initiated, reaches a steady value after a length of time that depends on the stirring rate. When equilibrium conditions are reached the pressure stays constant for hours indicating that no hydrogen consuming reaction takes place as is the case of nitrate melts [15].

Table 1 summarizes the results of the solubility experiments. Each value of the Henry's constant is the average of at least three different runs. The reproducibility of the results was within 5–7%.

The heat of solution $[\Delta H = -R\delta \ln K/(1/T)]$ computed from the slope of the plot $\log K$ versus $1/T$ is 8·2 kJ mol^{-1}.

The Henry's constants at 523 K, the heats and standard entropies of solution for hydrogen and water in acetates and nitrates are compared in Table 2. The standard entropies of solution have been computed by using the equation

Table 1. Values of the Henry's constants for hydrogen solubility at different temperatures

T (K)	$K \times 10^6$ (mol m^{-3} Pa^{-1})
529·6	3·25
547·6	3·39
565·9	3·69
573·3	3·71

$$\Delta S = \Delta H/T + R \ln (C_s/C_g)$$

where C_s and C_g are the concentrations in solution and in the gas phase, respectively. In view of the choice of standard states for both the gas and the solution (mol per unit volume) the ΔS values are uniquely a function of the interactions between the gas and the solvent ions [15–20].

From Table 2 it may be seen that in both melts hydrogen is about one thousand times less soluble than water. The heats of solution are relatively high and negative for water, and positive and low for hydrogen. This is consistent with the theory of gas solubility in molten salts which predicts a high solubility and a negative ΔH for interacting gases such as water, and a low solubility and a positive ΔH for a non-polar gas.

In the last case, in fact, the gas–solvent ion interactions are weak and the main energy contribution to the solubilization process is the work done against the surface tension of the melt to create a hole to accommodate the molecule.

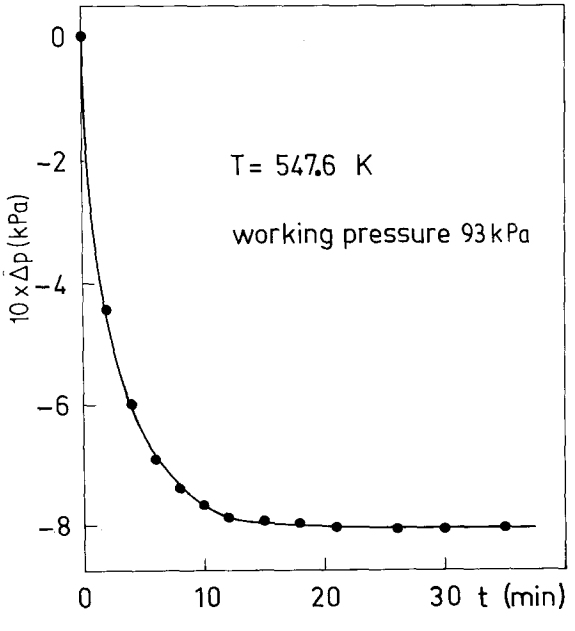

Fig. 1. Typical pressure decay during a solubility experiment.

Table 2. Thermodynamic parameters for gas solubilities in molten acetates and nitrates

Solute	*Solvent*	*Composition*	K_{523} (mol m^{-3} Pa^{-1})	H (kJ mol^{-1})	S_{523} (J K^{-1} mol^{-1})	*Reference*
H_2	(Na, K) acetates	46·3–53·7	$3{\cdot}16 \times 10^{-6}$	8·2	−19·8	this work
H_2O	(Na, K) acetates	46·3–53·7	$1{\cdot}24 \times 10^{-2}$	−43	−49	14
H_2	(Na, K) nitrates	50–50	$1{\cdot}39 \times 10^{-6}$	14	−16	15
H_2O	(Na, K) nitrates	50–50	$0{\cdot}94 \times 10^{-2}$	35	−37	20

The ΔS value for hydrogen solubility in acetates, as well as in nitrates, is lower than the corresponding value for water. As a negative entropy is indicative of a certain structuring of the solvent ions surrounding the gas molecule a lower ΔS is expected for a non-polar gas such as hydrogen. The thermodynamic data for hydrogen in acetates and nitrates are comparable. The solubility is, however, slightly higher in the first solvent as is the case for water. Because the energy involved in the hydrogen solubilization is mainly due to the work necessary to create a hole, the difference between acetates and nitrates has to be related to a lower surface tension of the acetates. To the best of our knowledge, the only surface tension data for acetates is relative to molten CH_3COOK at 588 K for which a value of 0·042 N m^{-1} is reported [21]. This value is, however, much lower than the corresponding value for molten KNO_3 (0·111 N m^{-1} at 588 K).

Lack of data for mixtures of acetates prevents any comparison of the experimental parameters with the theory [15–20].

The gas volumetric method used for the determination of the solubility of hydrogen cannot be used for acetic acid because this compound undergoes partial dimerization in the gas phase. Rough values for the solubility of acetic acid have been obtained either by titrating the acid stripped from saturated melts and collected on water or by comparing the limiting diffusion currents for the reduction of acetic acid and water and assuming equal diffusion coefficients [13, 14]. The data obtained, although too imprecise to be quoted, are sufficient to state that the solubility of acetic acid is of the same order of magnitude of the solubility of water (K about 10^{-2} mol m^{-3} Pa^{-1}). Further work is in progress in this direction.

3.2. *Hydrogen and acetic acid voltammetry*

Fig. 2 shows a cyclic voltammogram obtained with a platinum electrode in a partially wet melt saturated with hydrogen at a pressure of 90 kPa. The overall electrode reactions for waves A–B may be written [13]

$$H_2 \overset{CH_3COO^-}{\rightleftharpoons} 2\,CH_3COOH + 2\,e \qquad (1)$$

waves C–D correspond to the reaction

$$H_2O + e = \tfrac{1}{2}\,H_2 + OH^- \qquad (2)$$

as reported in [14].

The hydrogen oxidation wave is not affected by the water content of the melt if the potential scan is initiated in the positive direction. If the initial scan direction is reversed the general shape of the waves remains the same apart from a slight shift of the peak potentials in the cathodic direction. The shape of the cyclic voltammograms and of the polarograms at platinum electrodes for hydrogen oxidation depends on the state of the electrode surface. When the electrode is not very 'clean' the voltammograms with a vibrating electrode [22] are distorted by a maximum, the cyclic voltammograms are broad and the current does not decay properly after the maximum. 'Clean' electrode surfaces have been obtained by applying the procedure described in [14]. Before each measurement, in addition, the electrode was polarized several times within the potential region of interest.

The best results have been obtained by constructing the voltammograms from current–time curves traced at different potentials and measuring the currents at a fixed time, generally five seconds, after the application of the potential step [23] (Fig. 3).

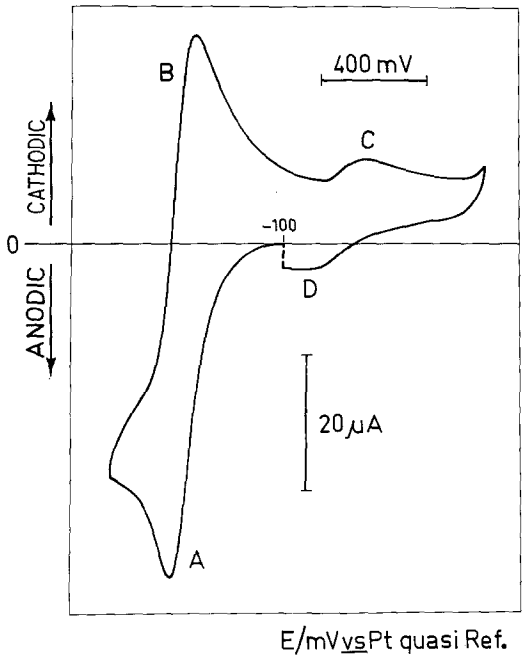

Fig. 2. Cyclic voltammogram obtained at a platinum electrode in a partially wet (Na, K) acetate melt saturated with hydrogen at a pressure of 90 kPa. Platinum electrode area about 7×10^{-6} m^2; temperature 250° C; scan rate 0·1 V s^{-1}.

Within the limits of experimental error (no correction has been made for the cylindrical shape of the electrode) the product $it^{1/2}$ is constant for times up to five seconds and the limiting currents in the constructed voltammograms are linearly dependent on the hydrogen partial pressure (Fig. 4) thus indicating that the process is diffusion controlled.

The reproducibility of the results obtained with this method can probably be ascribed to the state of the electrode surface which is always the same before the application of the potential steps.

If Reaction 1 is reversible and diffusion controlled the Nernst equation may be written [24]

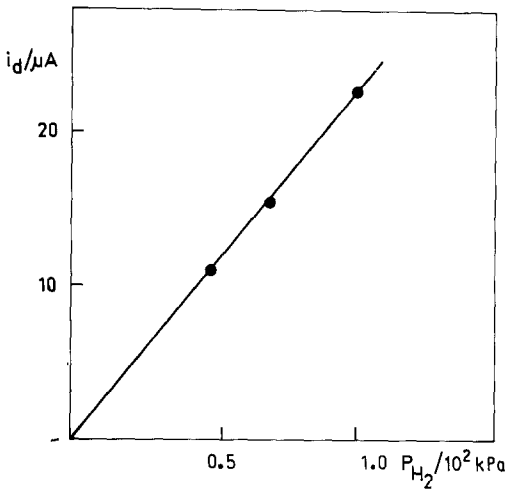

Fig. 4. Hydrogen pressure dependence of the limiting currents in the constructed voltammograms. Temperature 250° C. Platinum electrode area 7×10^{-6} m^2.

$$E = E_{1/2} + RT/2F \ln (-i)^2/(-i_d + i)$$

from which it can be seen that a plot of E versus $\ln(-i)^2/(-i_d + i)$ should be linear with slope equal to $RT/2F$ and that $E_{1/2}$ should depend on the hydrogen partial pressure (or concentration) following the equation

$$E_{1/2} = E' + RT/2F \ln p_{H_2}$$

where E' is a formal standard potential.

In Fig. 5 is shown the log plot for the wave in Fig. 3. It can be seen that the plot is linear with a reciprocal slope equal to 53·9 mV (theoretical slope at 250° C, 51·8 mV). Linear plots with slopes close to the theoretical are obtained only if the electrode is accurately cleaned. If this condition is not realized the diagrams are still linear with slopes much higher than the theoretical. Due to the uncertainty in the reference electrode potential, no plots of $E_{1/2}$ versus log

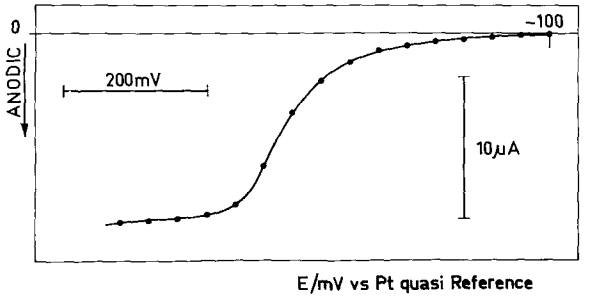

Fig. 3. Constructed voltammogram for hydrogen oxidation. Current measured at five seconds. Hydrogen partial pressure 46 kPa. Platinum electrode area 7×10^{-6} m^2. Temperature 250° C.

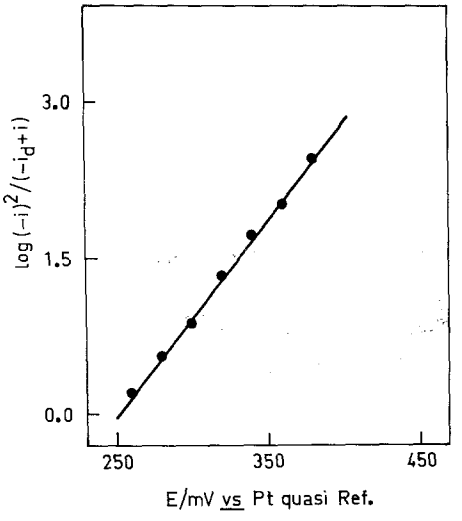

Fig. 5. Plot log $(-i)^2/(-i_d + i)$ versus E for the oxidation wave in Fig. 3. Reciprocal slope 53·9 mV (theoretical at 250° C, 51·9 mV).

p_{H_2} can be reported. Qualitatively it has been observed that the entire wave moves, as expected, toward more anodic potentials with increasing partial pressure.

The above results demonstrate that, at least on the time scale of a constructed polarogram, the oxidation of hydrogen is a reversible diffusion-controlled process at bright platinum electrodes. Detailed investigations on the mechanism of the hydrogen electrode are beyond the aim of this paper. It seems, however, worthwhile to point out that under these conditions it is impossible to specify any kinetic step for Reaction 1 that is normally discussed in terms of the Tafel–Volmer scheme [25]

$$H_2 + 2\,M = 2\,MH \quad \text{(Tafel)} \qquad (3)$$

$$2\,MH + 2\,B = 2\,M + 2\,HB + 2e \quad \text{(Volmer)} \qquad (4)$$

where M is the electrode and B a base.

Some information on the reaction path may, however, be deduced from the cyclic voltammetric data. Among the different electrode materials tested, only on platinum it was possible to obtain oxidation waves like the one shown in Fig. 2. This is not surprising in view of the role played by platinum in the hydrogen electrode reaction. Other electrode materials, such as glassy carbon, gold and tungsten, appear to be usable, especially the first two, in molten acetates. The background currents are greater than on platinum and only very broad and drawn-out waves are obtained in the presence of hydrogen and water.

The modifications of the oxidation curves at platinum with increasing scan rate give further information. At low scan rates (up to about 1 V s^{-1}) the oxidation curve is peak-shaped while, at faster sweep rates, it assumes progressively the shape of a wave. At the same time the current function $i_p/v^{1/2}$ decreases due to the presence of a preceding chemical reaction [26], the curve moves towards more anodic potentials and the peak width and separation increase.

This behaviour is consistent with the kinetic scheme discussed by Saveant and Vianello [27] in which the depolarizer is produced by dissociation (monomerization) of an electrochemically inactive dimer. If this mechanism is applicable to the present case, it may be concluded that, when the time scale of the experiment decreases, the rate-determining step is the formation of hydrogen atoms on the electrode surface which may occur only at a certain rate.

At low scan rates (less than 0·1–0·2 V s^{-1}) the half peak width, the peak separation and the ratio i_f/i_r are in reasonable agreement with the diagnostic criteria of Saveant and Vianello for the above mechanism and with those given by Shuman [28] who computed the theoretical cyclic voltammograms for a reversible monomerization following a reversible charge transfer. The two

Table 3. Typical cyclic voltammetric parameters for the oxidation of hydrogen and reduction of acetic acid in molten (Na, K) acetates at 250° C. Hydrogen pressure 95 kPa, acetic acid partial pressure 0·56 kPa. The theoretical values [26, 27] are given in parentheses. Scan rate 0·1 V s^{-1}; platinum electrode area about 7 × 10^{-6} m^2

Solute	*Half-peak width* (mV)	*Peak separation* (mV)	i_f/i_r
H_2	80 (75·2)	85 (79·5)	1·04 (1·09)
acetic acid	71 (70·3)	130 (78·9)	0·65 (0·95)

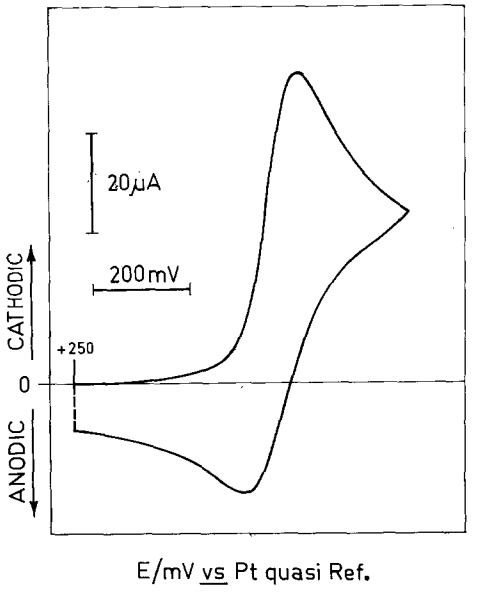

Fig. 6. Cyclic voltammogram for acetic acid reduction. Platinum electrode area about 7×10^{-6} m^2; temperature 250° C; acetic acid concentration unknown; scan rate 0·136 V s^{-1}.

mechanisms lead to the same curve when the overall reaction is diffusion controlled.

Typical parameters for the oxidation of hydrogen are given in Table 3. The diffusion coefficient for hydrogen, computed from the slope of the plot i_d versus p_{H_2} using the Cottrell equation and the determined Henry's constant at 523 K is 5×10^{-8} m^2 s^{-1} significantly larger than the value found for water in the same melt ($D = 1{\cdot}34 \times 10^{-9}$ m^2 s^{-1}) and comparable with the one reported in molten carbonates ($D = 4{\cdot}4 \times 10^{-8}$ m^2 s^{-1}) at much higher temperature [29].

In molten nitrates, where the hydrogen oxidation occurs only in the presence of hydroxide with a rather complex mechanism [11], the estimated diffusion coefficient is $D \lesssim 7{\cdot}8 \times 10^{-9}$ m^2 s^{-1} at 523 K.

The results obtained in solutions of hydrogen have been complemented by those obtained in solutions of acetic acid in the same melt. Figs. 6 and 7 show a cyclic voltammogram and a constructed polarogram for acetic acid reduction. Fig. 8 shows the pertinent logarithmic plot for the wave in Fig. 7. It can be seen that the plot is linear with a slope of 52·2 mV very close to the theoretical value of 51·9 mV at 523 K [24].

The shape of the cyclic voltammograms and

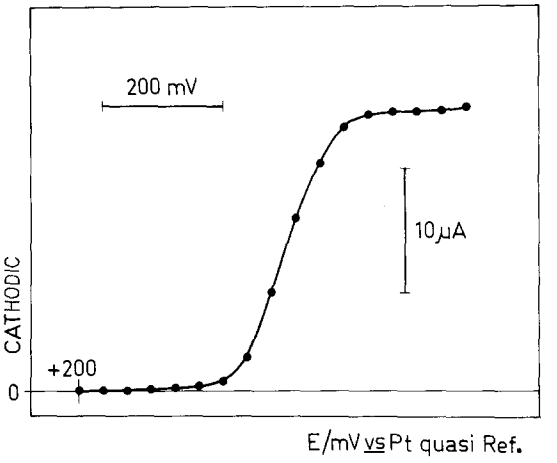

Fig. 7. Constructed voltammogram for acetic acid reduction. Platinum electrode area about 7×10^{-6} m^2; temperature 250° C; acetic acid concentration unknown.

the logarithmic analysis of the polarograms suggest, as is expected from the results obtained with hydrogen, that the reduction of acetic acid is a reversible diffusion-controlled process. The cyclic voltammetric parameters for the reduction of acetic acid summarized in Table 3 indicate, at low scan rate, a non-unity reaction order corresponding to the overall electrode reaction

$$2\ CH_3COOH + 2\ e = H_2 + 2\ CH_3COO^- \quad (5)$$

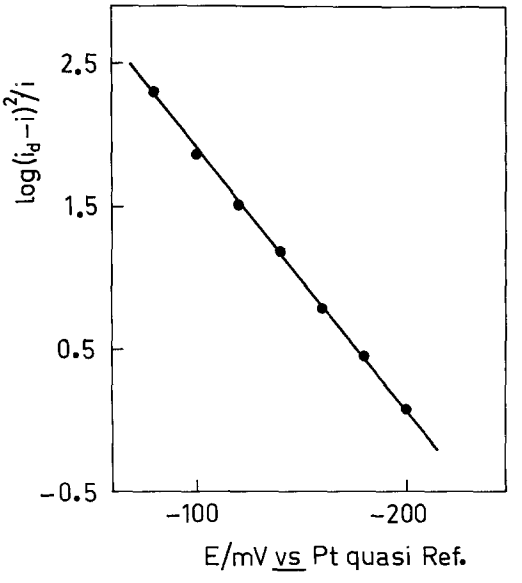

Fig. 8. Plot log $(i_d - i)^2/i$ versus E for the reduction wave in Fig. 7. Reciprocal slope 52·2 mV (theoretical at 250° C, 51·9 mV).

treated for cyclic voltammetry by Saveant and Vianello [27] and by Shuman [28]. For scan rates up to 5 V s^{-1} the peak width is in agreement with the theory while the current function $i_p/v^{1/2}$ decreases slightly indicating a possible CE behaviour. The ratio i_f/i_r, as well as the peak separation, are generally greater than those expected at any scan rate. Both facts may, however, be tentatively explained with the partial loss of hydrogen from the diffusion layer caused by the large solubility difference between hydrogen and acetic acid.

As for hydrogen oxidation, Reaction 5 may be discussed in terms of the Tafel–Volmer scheme (Equations 3 and 4). The above electrochemical results indicate, however, that in this melt the dimerization of hydrogen atoms is fast and reversible. This is not the case for the reduction of HCl in chloride melts [6–8] where the charge transfer step is faster than the hydrogen atom combination reaction and the electrode reaction does not involve molecular hydrogen.

No diffusion coefficient may be quoted for acetic acid because its solubility in the melt is, at present, not known.

Acknowledgements

This work was supported partially by the Italian National Council (CNR). The assistance of Dr Paola Rappanello with some of the measurements and the interest of Professor Mario Fiorani are gratefully acknowledged.

References

[1] B. S. Baker, 'Hydrocarbons Fuel Cell Technology', Academic Press, New York (1965), p. 194.
[2] H. W. Breiter, 'Electrochemical Processes in Fuel Cell', Springer Verlag, New York (1969), p. 217.
[3] W. Violstich, 'Fuel Cells', J. Wiley, London (1970).
[4] S. Pizzini and R. Morlotti, *Electrochim. Acta* **10** (1965) 1033.
[5] J. Goret, *Bull. Soc. Chim. France* (1964) 1074.
[6] Y. Kanzaki and M. Takahashi, *J. Electroanalyt. Chem.* **58** (1975) 349.
[7] N. Q. Minh and B. J. Welch, *Austr. J. Chem.* **28** (1975) 965.
[8] *Idem, ibid* **28** (1975) 2579.
[9] G. Letisse and B. Tremillon, *J. Electroanalyt. Chem.* **17** (1968) 387.
[10] B. Tremillon, A. Bernard and R. Molina, *ibid* **74** (1976) 53.
[11] E. Desimoni, F. Palmisano and P. G. Zambonin, *ibid* **84** (1977) 323.
[12] E. Desimoni, F. Paniccia, L. Sabbatini and P. G. Zambonin, *J. Appl. Electrochem.* **6** (1976) 445.
[13] R. Marassi, V. Bartocci and F. Pucciarelli, *Talanta* **19** (1972) 203.
[14] R. Marassi, V. Bartocci, F. Pucciarelli and P. Cescon, *J. Electroanalyt. Chem.* **47** (1973) 509.
[15] E. Desimoni, F. Paniccia and P. G. Zambonin, *J. Chem. Soc. Far. Trans. I* **69** (1973) 2014.
[16] M. Blander, W. R. Grimes, N. V. Smith and G. M. Watson, *J. Phys. Chem.* **63** (1962) 1164.
[17] G. M. Watson, R. B. Evans, W. R. Grimes and N. V. Smith, *J. Chem. Eng. Data* **7** (1962) 285.
[18] B. Clever and D. E. Mather, *Trans. Faraday Soc.* **66** (1970) 2469.
[19] P. E. Field and W. J. Green, *J. Phys. Chem.* **75** (1971) 821.
[20] P. G. Zambonin, V. L. Cardetta and S. Signorile, *J. Electroanalyt. Chem.* **28** (1970) 237.
[21] G. J. Janz 'Molten Salts Handbook', Academic Press, New York, London (1967), p. 82.
[22] F. Schiavon, G. A. Mazzocchin and G. G. Bombi, *J. Electroanalyt. Chem.* **29** (1971) 401.
[23] R. W. Murray, in 'Techniques in Chemistry' Vol. I, Part IIA, (Eds. Weisberger and B. W. Rossiter) Wiley-Interscience, New York (1971) p. 600.
[24] G. Raspi, F. Pergola and D. Cozzi, *J. Electroanalyt. Chem.* **15** (1967) 35.
[25] J. O'M. Bockris and A. K. N. Reddy, in 'Modern Electrochemistry' Vol. II, Plenum Press, New York (1970), pp. 1231–50.
[26] R. S. Nickolson and I. Shain, *Analyt. Chem.* **37** (1965) 178.
[27] J. M. Saveant and V. Vianello, *Electrochim. Acta* **12** (1967) 1545.
[28] M. S. Shuman, *Analyt. Chem.* **42** (1970) 521.
[29] M. A. Vogin, A. L. Lvov and V. A. Laskutin, *Elektrokhimija* **9** (1973) 368.